A Simple Method for Calculating Quantum Effects on the Temperature Dependence of Bimolecular Reaction Rates: Application to $H_2 + H \rightarrow H + H_2$ and $CH_4 + H \rightarrow CH_3 + H_2$

David Z. Goodson,*,† Dustin W. Roelse,† Wan-Ting Chiang,† Steven M. Valone,‡ and J. D. Doll§

Contribution from the Department of Chemistry, Southern Methodist University, Dallas, Texas 75275, Materials Science and Technology Division, MST-8, Los Alamos National Laboratory, Los Alamos, New Mexico 87545, and Department of Chemistry, Brown University, Providence, Rhode Island 02912

Received February 24, 2000. Revised Manuscript Received July 11, 2000

Abstract: The temperature dependence of thermal rate constants for hydrogen atom abstraction reactions is studied using transition-state theory with temperature-dependent effective potential energy functions derived from a quantum mechanical path integral analysis with a low-temperature correction. The theory uses temperature-dependent activation energies determined from Gaussian averages of an empirical potential. Simple analytic expressions are obtained for rate constants. To test the theory the rate constant for $H_2 + H$ is calculated, and the predicted curvature of the Arrhenius plot is shown to agree with results from accurate quantum scattering calculations. The predicted curvature for $CH_4 + H$ is compared with experimental results and shown to give better agreement with the observed temperature dependence than do commonly used empirical fits. The expression $k(T) = aT \exp[-(E_0 + E_1T_{eff}^{-1} + E_2T_{eff}^{-3/2})/RT]$, with $T_{eff} = T + T_0$, is suggested for the rate constant for $CH_4 + H$, with the parameters a, E_0, E_1, E_2, and T_0 obtained from theory rather than by fitting to the experimental reaction rates.

I. Introduction

The rigorous quantum mechanical calculation of a chemical reaction rate is a daunting challenge. It requires an accurate ab initio potential energy surface and then a solution of the difficult quantum scattering equations for the dyanmics of the nuclei. This has been accomplished in benchmark calculations for a few simple systems.[1] However, in practical applications such as, for example, computer simulations of hydrocarbon combustion,[2,3] it is more typical simply to use empirical expressions with parameters that are fit directly to experimentally determined reaction rates. We develop here a semiempirical quantum-mechanical description of reaction rates. Instead of an ab initio potential surface, we use an empirical surface parametrized to fit molecular atomization energies and spectroscopic data.[4] To describe the quantum dynamics we propose a simple semiclassical procedure that interpolates between known high- and low-temperature limits.

In the limit $T \rightarrow \infty$, it is possible to rigorously derive semiclassical descriptions of the dynamics. A particularly convenient approach is the effective potential approximation developed by Feynman,[5] in which the true potential surface, V, is transformed to a T-dependent effective potential, $V_{eff}(T)$, which can then be treated with classical mechanics. Although an improvement over a purely classical description, the effective potential approach can be somewhat inaccurate at intermediate T, which in practice is the range of particular interest. One way to extend the validity of the theory is to use a more sophisticated version of the analysis,[6,7] but this can obscure the appealing physical picture given by Feynman's approach. We propose a very minor modification of the Feynman expression, in which an empirical parameter is included to improve the accuracy at low T. This theory remains correct at $T \rightarrow \infty$, it gives the correct result at $T = 0$ K, and it preserves the straightforward mathematical structure and elegant qualitative picture of the effective quantum potential.

We will demonstrate this approach in the context of transition-state theory (TST). This will provide a test of the accuracy of the theoretical ideas. In addition, it will yield simple analytical expressions for bimolecular rate constants that could be used in combustion studies in place of the purely empirical expressions. An important goal of reaction rate theory is the determination of temperature dependences of rate constants. The Arrhenius expression,

$$k = A \exp(-E_a/RT) \tag{1}$$

where E_a is the activation energy and R is the gas constant, is often not sufficient for quantitative descriptions.[8] E_a is usually

† Southern Methodist University.
‡ Los Alamos National Laboratory.
§ Brown University.

(1) Schatz, G. C. *J. Phys. Chem.* **1996**, *100*, 12839−12847. Miller, W. H. *J. Phys. Chem. A* **1998**, *102*, 793−806 and references therein.
(2) Glassman, I. *Combustion*; Academic Press: San Diego, 1996; p 553.
(3) *GRI-Mech 3.0*; Gas Research Institute, 1999; http://www.me.berkeley.edu/gri_mech.
(4) Brenner, D. W. *Phys. Rev. B* **1990**, *42*, 9458−9471; **1992**, *46*, 1948.
(5) Feynman, R. P.; Hibbs, A. R. *Quantum Mechanics and Path Integrals*; McGraw-Hill: New York, 1965; pp 268−298. Feynman, R. P. *Statistical Mechanics*; Benjamin, New York, 1972; pp 72−96.
(6) Gillan, M. J. *Philos. Mag. A* **1988**, *58*, 257−283. Voth, G. A.; Chandler, D.; Miller, W. H. *J. Chem. Phys.* **1989**, *91*, 7749−7760.
(7) Jang, S.; Voth, G. A. *J. Chem. Phys.* **1999**, *111*, 2357−2370, 2371−2384; **2000**, *112*, 8747−8757.
(8) Wayne, R. P. In *The Theory of Chemical Kinetics*; Bamford, C. H., Tipper, C. F. H., Eds.; Comprehensive Chemical Kinetics 2; Elsevier: Amsterdam, 1969; pp 189−301 and references therein.

10.1021/ja000674+ CCC: $19.00 © 2000 American Chemical Society
Published on Web 09/09/2000

treated as if it were independent of temperature, and any deviation from linear behavior in the plot of log k vs $1/T$ is attributed to temperature dependence in A. Classical collision theory suggests only a weak temperature dependence of the preexponential factor, of the form $A \propto T^{1/2}$, while theoretical arguments based on TST with corrections for quantum mechanical tunneling[8−10] can predict significantly different dependences. Our effective quantum potential transition-state theory (EQPTST) will use a standard TST expression for A but will include quantum effects such as tunneling and zero-point energy through the T dependence of the effective potential.

First we will present results for the hydrogen exchange reaction

$$H_2 + H \rightarrow H + H_2 \tag{2}$$

This has previously been the subject of rigorous quantum mechanical calculations and therefore is a good test case for our simple approximate theory. Then we will consider the reaction

$$CH_4 + H \rightarrow CH_3 + H_2 \tag{3}$$

for which there exists an extensive literature of theoretical and experimental studies[11−23] on account of its importance as an elementary reaction in hydrocarbon pyrolysis and combustion.

II. Method

1. Quantum Theory. Feynman's semiclassical analysis is based on his path-integral formulation of quantum statistical mechanics. The equation for the statistical density matrix is formally identical to that for the kernel that expresses the time dependence of the wave function of a quantum mechanical particle over a time interval that is taken to be negative and imaginary. Thus, calculations in statistical mechanics can be carried out using path-integral techniques of quantum dynamics. To calculate the partition function from the statistical density matrix, it is sufficient to consider only paths that return to their starting point. The integrals that need to be evaluated are very difficult to evaluate on account of the need to describe the many possible paths. However, if T is sufficiently large then one can derive a simple approximate expression for the canonical partition function, Z.[5] For a system described by the Hamiltonian $-\hbar^2/2m\ d^2/dx^2 + V(x)$, the result is

$$Z = \left(\frac{mk_BT}{2\pi\hbar^2}\right)^{1/2} \int e^{-V_{eff}(x)/k_BT}\, dx \tag{4}$$

where k_B is the Boltzmann constant and

$$V_{eff}(x) = \frac{1}{\sqrt{2\pi\sigma^2}} \int_{-\infty}^{\infty} V(x+z)\, e^{-z^2/2\sigma^2}\, dz \tag{5}$$

$$\sigma^2 = \frac{\hbar^2}{12mk_BT} \tag{6}$$

The significance of this result is the fact that eq 4 has exactly the form of the *classical* partition function, except that V is replaced by the effective potential V_{eff}, which is just a Gaussian average of V with a temperature-dependent standard deviation σ. This implies, for calculations in statistical mechanics, that an approximate quantum result can be obtained simply by using V_{eff} in place of V in an otherwise classical calculation.

It has been suggested[24] that classical dynamics on the potential V_{eff} could be used to simulate quantum dynamics on the true potential V. For example, it was shown[24] that when V_{eff} is used in place of V in TST for the rate constant with a one-dimensional barrier, one obtains the standard Wigner tunneling correction. This approach can be derived from a path-integral analysis as an approximation to centroid TST.[25] It has been used to describe the diffusion of H on a Cu surface,[26] and the results were later found to agree with those from an elaborate reaction-path variational TST calculation with semiclassical adiabatic tunneling corrections.[27]

EQPTST provides an appealing qualitative model for quantum effects. At a minimum of V, averaging over neighboring points with eq 5 will increase the potential energy. This accounts for the fact that the minimum of V is, in practice, inaccessible to the system on account of the impossibility of localizing a quantum mechanical particle. In effect, the averaging provides a zero-point energy correction. At a maximum of V the averaging reduces the potential energy. In effect, this is a tunneling correction. At a saddle point of V, averaging over a given coordinate z_i will reduce the potential if $\partial^2V/\partial z_i^2$ is negative and increase it if $\partial^2V/\partial z_i^2$ is positive. Elsewhere, V can be approximated as a linear function, in which case the averaging in eq 5 will have little effect. At high T the quantum effects will be small, because if the average kinetic energy is large then only rarely will a particle have a low enough kinetic energy that the difference between V and V_{eff} will significantly affect the dynamics. Accordingly, the standard deviation given by eq 6 goes to zero in the limit of infinite T.

At $T = 0$ K, the system, according to classical mechanics, will be at rest at the nearest minimum of V. The quantum mechanical energy of the system will be the value of V at this minimum plus a zero-point energy correction. A minimum of V_{eff} corresponds to a stable chemical species, for which the zero-point energy can be determined empirically from analysis of the vibrational spectrum. This suggests that we replace T in eq 6 with an effective temperature, given by some function $T_{eff}(T)$ subject to the contraints

$$\lim_{T\rightarrow\infty} T_{eff}(T) = T, \qquad T_{eff}(0) = T_0 \tag{7}$$

where T_0 is a constant chosen such that eq 5 at $T = 0$ K reproduces the empirical zero-point energy of a known species.

As an illustration of this interpolation between high- and low-temperature limits, consider a one-dimensional harmonic oscillator of mass m and frequency ω. In this case, the exact quantum mechanical partition function is obtained if in eq 5 we substitute for σ^2 the expression[28]

(9) Johnston, H. S. *Gas-Phase Reaction Rate Theory*; Ronald Press: New York, 1966; pp 101−252, 321−328.
(10) Moore, J. W.; Pearson, R. G. *Kinetics and Mechanisms*; John Wiley & Sons: New York, 1981; pp 158−213.
(11) Clark, T. C.; Dove, J. E. *Can. J. Chem.* **1973**, *51*, 2147−2154.
(12) Shaw, R. *J. Phys. Chem. Ref. Data* **1978**, *7*, 1179−1190 and references therein.
(13) Tsang, W.; Hampson, R. F. *J. Phys. Chem. Ref. Data* **1986**, *15*, 1087−1279.
(14) Schatz, G. C.; Walch, S. P.; Wagner, A. F. *J. Chem. Phys.* **1980**, *73*, 4536−4547.
(15) Joseph, T.; Steckler, R.; Truhlar, D. G. *J. Chem. Phys.* **1987**, *87*, 7036−7049.
(16) Lu, D.; Maurice, D.; Truhlar, D. G. *J. Am. Chem. Soc.* **1990**, *112*, 6206−6214.
(17) Truong, T. N. *J. Chem. Phys.* **1994**, *100*, 8014−8025.
(18) Walker, R. W. *J. Chem. Soc. (Ser. A)* **1968** 2391−2398.
(19) Sepehrad, A.; Marshall, R. M.; Purnell, H. *J. Chem. Soc., Faraday Trans. 1* **1979**, *75*, 835−843.
(20) Baulch, D. L.; Cobos, C. J.; Cox, R. A.; Esser, C.; Frank, P.; Just, Th.; Kerr, J. A.; Pilling, M. J.; Troe, J.; Walker, R. W.; Warnatz, J. *J. Phys. Chem. Ref. Data* **1992**, *21*, 412−734.
(21) Kurylo, M. J.; Timmons, R. B. *J. Chem. Phys.* **1969**, *50*, 5076−5082.
(22) Kurylo, M. J.; Hollinden, G. A.; Timmons, R. B. *J. Chem. Phys.* **1970**, *52*, 1773−1781.
(23) Rabinowitz, M. J.; Sutherland, J. W.; Patterson, P. M.; Klemm, R. B. *J. Phys. Chem.* **1991**, *95*, 674−681.
(24) Doll, J. D. *J. Chem. Phys.* **1984**, *81*, 3536−3541.
(25) Voth, G. A. *J. Chem. Phys.* **1991**, *94*, 4095−4096.
(26) Valone, S. M.; Voter, A. F.; Doll, J. D. *Surf. Sci.* **1985**, *155*, 687−699; *J. Chem. Phys.* **1986**, *85*, 7480−7486; *J. Chem. Phys.* **1987**, *87*, 2407.
(27) Lauderdale, J. G.; Truhlar, D. G. *J. Am. Chem. Soc.* **1985**, *107*, 4590−4591.
(28) Doll, J. D.; Myers, L. E. *J. Chem. Phys.* **1979**, *71*, 2880−2883.

$$\sigma_{HO}{}^2 = \frac{2k_B T}{m\omega^2}\ln\left[\frac{\sinh(\hbar\omega/2k_B T)}{\hbar\omega/2k_B T}\right] \quad (8)$$

We can make the high-temperature σ^2, given by eq 6, agree quite well with $\sigma_{HO}{}^2$ at low T by simply substituting $T_{eff} = T + T_0$ for T in eq 6 with $T_0 = \hbar\omega/12k_B$. Figure 1 shows that this substitution significantly improves the accuracy of the high-temperature formalism of eqs 4 and 5.

Molecular potential energy surfaces are, of course, anharmonic. In particular, the potential energy of a diatomic molecule is steeper for compressing the bond than it is for stretching the bond. The use of $\sigma_{HO}{}^2$ to describe the spread of the quantum averaging gives equal weight to bond compression and stretching. In reality, quantum excursions are less likely to venture into steeper regions. Therefore, use of a symmetric probability distribution overestimates the zero-point energy, which yields too small a value for the bond energy. This problem is even worse if the high-T distribution, eq 6, is used. That result comes from an analysis in which the effect of the potential energy on the probability of a given quantum excursion is ignored completely. Hence, the high-T analysis leads to an even smaller value for the bond energy. We wish to avoid the computational complexity of an analysis in which σ^2 depends on V. However, since we expect that a more accurate treatment of the quantum mechanics would give a slightly smaller bond energy, we will mimic this effect by using eq 6 with a functional form for T_{eff} consistent with the limits given by eqs 7 but that at intermediate T gives a value of σ^2 that is slightly smaller than $\sigma_{HO}{}^2$. The class of functions

$$T_{eff}{}^{(\gamma)} = (T^{1/\gamma} + T_0{}^{1/\gamma})^{\gamma} \quad (9)$$

characterized by the free parameter γ, with $\gamma > 1$, satisfies these criteria.

2. Application to H + H_2. The minimum-energy activated complex for this reaction is linear. Therefore, we will treat this as a problem in two degrees of freedom, in terms of the collinear bond distances x and y. For V we use Brenner's potential I,[4] which is a sum of two-body interactions with perturbations from nearby atoms. For H + H_2 it has the form

$$V(x,y) = V_{HH}(x;y) + V_{HH}(y;x) \quad (10)$$

In V_{HH}, the first argument is the primary two-body coordinate, while the second argument describes the position of the neighboring atom. V_{HH} is the sum of repulsive and attractive potentials, in the form

$$V_{HH}(q;s) = f(q)\{D^{(R)}\exp[-\beta^{(R)}(q - q^{(e)})] - B(q,s)D^{(A)}\exp[-\beta^{(A)}(q - q^{(e)})]\} \quad (11)$$

This is a Morse function that has been modified by the functions f and B. $f(q)$ is a cutoff function that smoothly interpolates to zero at large q. B is a rather complicated function that models the effects of nearby atoms on the primary interaction.

The variance for the Gaussian averaging is given by

$$\sigma_{HH}{}^2 = \hbar^2/12\mu_{HH}k_B T_{eff,HH} \quad (12)$$

Note that the mass in eq 6 has been replaced by the reduced mass, $\mu_{HH} = m_H/2$. The effective potential is $V_{eff}(x,y) = \bar{V}_{HH}(x;y) + \bar{V}_{HH}(y;x)$, where

$$\bar{V}_{HH}(x;y) = \frac{1}{2\pi\sigma_{HH}{}^2}\int_{-\infty}^{\infty}\int_{-\infty}^{\infty} e^{-(z_x{}^2 + z_y{}^2)/2\sigma_{HH}{}^2} V_{HH}(x + z_x;y + z_y)\,dz_x\,dz_y \quad (13)$$

In principle, this integration ought to be performed in three-dimensional space, over vector displacements $\mathbf{z}_x$ and $\mathbf{z}_y$. However, we have found that integration in one-dimensional space is accurate enough, introducing significant error only for the very high energy configurations corresponding to small x or y. We will evaluate the integral using numerical quadrature. The value

$$T_{0,HH} = 513\ \text{K} \quad (14)$$

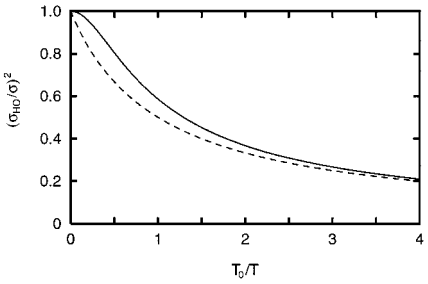

Figure 1. Ratio of Gaussian variance $\sigma_{HO}{}^2$, eq 8, for the one-dimensional harmonic oscillator to the Gaussian variance σ^2, eq 6, from the high-temperature analysis. The dashed curve shows the result from approximating $\sigma_{HO}{}^2$ with eq 6 but with $T + T_0$ substituted for T.

gives agreement with the spectroscopically determined zero-point energy of 6.29 kcal/mol for H_2.[29]

3. Application to Hydrocarbon Reactions. Now consider the reaction CH_4 + H. We will denote the reacting hydrogen of methane as H′ and the nonreacting hydrogens as H_a, H_b, and H_c. Let x be the C−H′ distance, let y be the H′−H distance, and let r_a, r_b, and r_c be the nonreacting C−H_α distances. The C−H′−H configuration is collinear along the reaction path. The angle between the reactive and nonreactive C−H bonds will be treated as a quadratic polynomial in x that interpolates between 109.5° for CH_4, 90° for CH_3, and 102.4° at x = 1.47 Å.[14]

The Brenner potential takes the form

$$V(x,y,r_a,r_b,r_c) = V_{CH'}(x;y,r_a,r_b,r_c) + V_{HH'}(y;x) + \sum_\alpha V_{CH_\alpha}(r_\alpha;x,r_\beta,r_\gamma) \quad (15)$$

with

$$V_{ij}(q;\mathbf{s}) = f_{ij}(q)\{D_{ij}{}^{(R)}\exp[-\beta_{ij}{}^{(R)}(q - q_{ij}{}^{(e)})] - B_{ij}(q,\mathbf{s})D_{ij}{}^{(A)}\exp[-\beta_{ij}{}^{(A)}(q - q_{ij}{}^{(e)})]\} \quad (16)$$

where q is the primary coordinate and $\mathbf{s}$ is the set of secondary coordinates. (In principle, eq 15 ought to contain in addition a term describing the H_a−H′ potentials, but these interactions are negligible along the entire course of the reaction path.) The secondary effects are relatively small. Therefore, it is possible to reduce the computational cost of the quadrature with little effect on the accuracy by introducing an approximation into the integration over secondary C−H distances. Consider the quadrature for $V_{CH'}$. The effective potential for the C−H′ interaction will require the integral

$$h_{H'}(x;\mathbf{r}) = (2\pi\sigma^2)^{-3/2}\int_{-\infty}^{\infty}\int_{-\infty}^{\infty}\int_{-\infty}^{\infty} B(x,r_a + z_a,r_b + z_b,r_c + z_c) \times e^{-(z_a{}^2 + z_b{}^2 + z_c{}^2)/2\sigma^2}\,dz_a\,dz_b\,dz_c \quad (17)$$

Only the case $r_a = r_b = r_c \equiv r$ will be of interest to us. If we replace B with its Taylor expansion in powers of the z_α, then

$$h_{H'}(x;r) = B(x,r,r,r) + 3\sigma^2\frac{1}{2}\frac{\partial^2 B}{\partial r_a{}^2}\Big|_{r_a = r} + O(\sigma^4)$$

$$= 3(2\pi\sigma^2)^{-1/2}\int_{-\infty}^{\infty} B(x,r + z,r,r)\,e^{-z^2/2\sigma^2}\,dz - 2B(x,r,r,r) + O(\sigma^4) \quad (18)$$

The notation $O(\sigma^4)$ means that the error from this approximation will be proportional to σ^4 in the limit of small σ. Similarly, the effective potential for the C−H_α interaction, with secondary nonreacting C−H distances set to r, will require the integral

(29) Huber, K. P.; Herzberg, G. *Molecular Spectra and Molecular Structure: IV. Constants of Diatomic Molecules*; Van Nostrand Reinhold: New York, 1979; p 250.

$$h_{H_\alpha}(r_\alpha;r,x) = 2(2\pi\sigma^2)^{-1/2}\int_{-\infty}^{\infty} B(r_\alpha,r+z,r,x)\, e^{-z^2/2\sigma^2}\, dz + (2\pi\sigma^2)^{-1/2}\int_{-\infty}^{\infty} B(r_\alpha,r,r,x+z)\, e^{-z^2/2\sigma^2}\, dz - 2B(r_\alpha,r,r,x) + O(\sigma^4) \quad (19)$$

Thus, the h functions can be computed with one-dimensional quadratures, reducing the calculation of V_{eff} from a four-dimensional quadrature to a two-dimensional one. For example, the effective potential for the C−H′ interaction is

$$\bar{V}_{CH'}(x;r) = (2\pi\sigma_{CH}{}^2)^{-1/2}\int_{-\infty}^{\infty} e^{-z^2/2\sigma_{CH}{}^2} h_{H'}(x+z;r)\, dz + O(\sigma_{CH}{}^4) \quad (20)$$

The physical meaning of this approximation is that, in calculating the effective potential for a primary C−H interaction, the only quantum fluctuations of secondary nonreacting C−H bonds that we will consider are those in which one of these bond distances fluctuates while the others remain fixed at their equilibrium values. In other words, for purposes of computing quantum effects on the activation energy, we are ignoring four-body effects while including all two- and three-body effects.

Note that we will need a different value of σ for a C−H bond than for an H−H bond, on account of the different values for the reduced mass and for T_0. The value

$$T_{0,CH} = 247\ K \quad (21)$$

gives agreement with the spectroscopically determined zero-point energy of 28.3 kcal/mol for CH_4.[30] There is a minor inconsistency in using the Brenner potential with an effective temperature for C−H bonds. For the C−H well depth, Brenner used the bond energy of the CH molecule without subtracting the zero-point energy.[4] Thus, we are, in a sense, adding zero-point energy to a potential that already includes it. We will assume that any errors from this procedure will be insignificant, since the quantum effects for C−H interactions are smaller than those for H−H interactions and because the rate analysis depends on an energy difference rather than on absolute atomization energies. However, in principle, one ought to reparametrize the potential using the correct well depth. For the H−H potential, Brenner did correct the H_2 well depth for zero-point energy.[4]

III. Results

1. $H_2 + H \rightarrow H + H_2$. This reaction is the standard test case for theoretical methods. Since it involves only H atoms the quantum effects will be relatively large, making this a stringent test for an approximate quantum theory.

We have calculated the temperature-dependent activation energy as the difference between V_{eff} evaluated at the linear H_3 saddle point and at the reactants well. The values are fit by the expression

$$E_a = 9.806\ \text{kcal mol}^{-1} - (2196\ \text{kcal mol}^{-1}\ \text{K})\tau + (5369\ \text{kcal mol}^{-1}\ \text{K}^{3/2})\tau^{3/2} \quad (22)$$

where $\tau = 1/T_{eff}$. The maximum error from eq 22 is ±0.005 kcal/mol for $T_{eff} > 670$.

Our strategy is to substitute $E_a(T_{eff}{}^{(\gamma)})/T$, with $T_{eff}{}^{(\gamma)}$ given by eq 9, into the Arrhenius expression, eq 1, while using an otherwise conventional reaction rate theory to determine the temperature dependence of the prefactor A. Empirical fits typically use the form[2,3,13,20,23]

$$A = aT^b \quad (23)$$

where a and b are adjustable parameters. In contrast, TST uses[10]

$$A \propto T^{1/2}\frac{Q_{t,H_3}Q_{r,H_3}Q_{v,\text{sym stretch}}Q_{v,\text{bend}}{}^2Q_{t,\text{antisym stretch}}}{Q_{t,H}Q_{t,H_2}Q_{r,H_2}Q_{v,H_2}} \quad (24)$$

in terms of partition functions Q_t, Q_r, and Q_v for translational, rotational, and vibrational motion, respectively. The temperature dependence of the partition functions is

$$Q_t \propto T^{3/2}, \quad Q_r \propto T, \quad Q_v = [1 - \exp(-\hbar\omega/k_BT)]^{-1}, \quad Q_{t,\text{antisym stretch}} \propto T^{1/2} \quad (25)$$

The TST expression for k is complicated by the dependence on the vibrational frequencies, ω_i, of the reactants and of the activated complex, but it can be simplified to the form of eq 23 through approximations. Expanding the Q_v about the high-T limit gives $b = {}^3/_2$, while taking the low-T limit of the Q_v gives $b = -{}^1/_2$.

Careful benchmark calculations for k are available for the case of zero total angular momentum ($J = 0$) from rigorous quantum scattering theory (QST)[31,32] or flux autocorrelation function calculations (FACF),[33] using a Born−Oppenheimer potential surface fit to ab initio electronic energies. Such calculations have also been carried out, approximately, for $J > 0$ and then the total rate constant obtained from a weighted sum over J.[31,33] (Our present analysis and those of refs 31−33 assume that the three H atoms are distinguishable. These results can be approximately related to indistinguishable-atom calculations[34] and to experimentally determined rate constants as described in ref 35.) Figure 2 compares the QST and FACF results for total rate constants with our results from TST with different expressions for the Gaussian variance. To emphasize the nonclassical curvature, we plot log k−log k_{cl}, where k_{cl} is the expression from classical collision theory,

$$k_{cl} = aT^{1/2}\, e^{-E_{a,\infty}/RT} \quad (26)$$

with a chosen so that $k_{cl} = 3.20 \times 10^{-13}$ cm^3 molecule^{-1} s^{-1} at 1000 K, which is the average of the QST and FACF results.[31,33] The solid curves use the full TST expression, which can be written as

$$k = \alpha T^{-1/2} f_r(T) f_v(T) \exp[-E_a(T_{eff}{}^{(\gamma)})/RT] \quad (27)$$

with

$$\alpha = 2k_Bh^2\left(\frac{3}{4\pi k_B m_H}\right)^{3/2} I_\infty{}^{\ddagger}/I_\infty{}^{(H_2)} \quad (28)$$

where the I_∞'s are the moments of inertia from the classical potential (i.e., at infinite T). The function

$$f_r(T) = 1 - 22.5\text{K}/T_{eff} \quad (29)$$

is an accurate fit to the weak T dependence of the ratio of moments of inertia that comes from the effects of the Gaussian averaging on the values of the bond distances. The function $f_v(T)$ is the ratio of the Q_v in eq 24, which we have evaluated

(30) Jones, L. H.; McDowell, R. S. *J. Mol. Spectrosc.* **1959**, *3*, 632−653.
(31) Colton, M. C.; Schatz, G. C. *Int. J. Chem. Kinet.* **1986**, *18*, 961−975.
(32) Chatfield, D. C.; Truhlar, D. G. *J. Chem. Phys.* **1991**, *94*, 2040−2044.
(33) Matzkies, F.; Manthe, U. *J. Chem. Phys.* **1997**, *106*, 2646−2653.
(34) Park, T. J.; Light, J. C. *J. Chem. Phys.* **1989**, *91*, 974−988.
(35) Truhlar, D. G. *J. Chem. Phys* **1976**, *65*, 1008−1010.

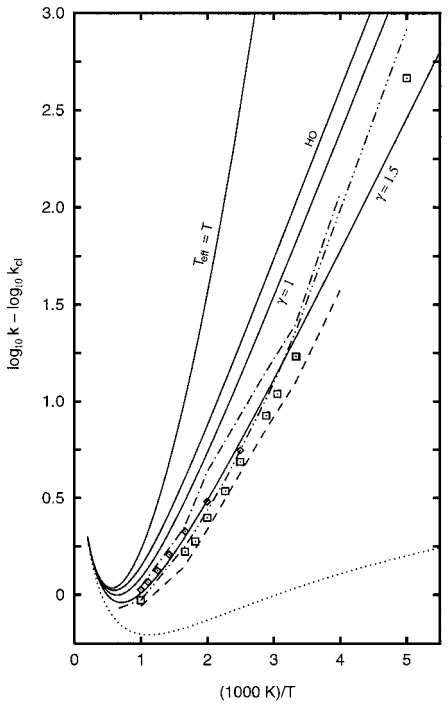

Figure 2. Difference between $\log_{10} k$ and $\log_{10} k_{cl}$ vs 1000 K/T for $H_2 + H \rightarrow H + H_2$, with k and k_{cl} in units of cm^3 molecule^{-1} s^{-1}. k_{cl} is the rate constant from classical collision theory, eq 26, with temperature-independent E_a and prefactor $a = 3.50 \times 10^{-14}$ cm^3 K$^{-1/2}$ molecule^{-1} s^{-1}. Diamonds indicate results from quantum scattering theory,[31] while squares indicate flux autocorrelation function results.[33] The solid curves show results from EQPTST, using eq 27 with the one-dimensional harmonic oscillator expression, eq 8 for σ^2, or with σ^2 given by eq 6 with T_{eff} equal to T or with T_{eff} given by eq 9 with the indicated value of the parameter γ. The dashed and the dash−dot curves correspond to conventional TST with a Wigner or Eckart tunneling correction, respectively.[37] The dash−dot−dot curve corresponds to variational TST with a multidimensional tunneling correction,[38] while the dotted curve shows conventional TST, eq 27, with classical temperature-independent activation energy.

using vibrational frequencies from ref 36. The dotted curve corresponds to conventional TST with the activation energy set to the constant $E_{a,\infty}$, which for the Brenner potential is 9.806 kcal/mol. The other three curves show results from representative TST treatments with tunneling corrections; specifically, the dashed and dash−dot curves are from conventional TST calculations by Espinosa-García et al.[37] using corrections of the Eckart or Wigner forms, respectively, while the dash−dot−dot curve is from the variational TST of Garrett et al.,[38] with a multidimensional semiclassical least-action tunneling correction and the same potential that was used in the QST and FACF calculations.

Our EQPTST with $\gamma = 1.5$ gives excellent agreement with the FACF and QST results at all temperatures except the lowest (250 K), where it gives a value that is somewhat too small. We find[39] that $\gamma = 1.5$ also gives excellent agreement with the exact rate constants with isotopic substitution of D for H. It is clear from eq 9 that the sensitivity of the results to the value chosen for γ decreases as T_0 decreases, and T_0 decreases as the atomic masses increase. Thus, even if 1.5 were not exactly the optimal

(36) Truhlar, D. G.; Horowitz, C. J. *J. Chem. Phys.* **1978**, *68*, 2466−2476.

(37) Espinosa-García, J.; Olivares del Valle, F. J.; Corchado, J. C. *Chem. Phys.* **1994**, *183*, 95−100.

(38) Garrett, B. C.; Truhlar, D. G.; Varandas, A. J. C.; Blais, N. C. *Int. J. Chem. Kinet.* **1986**, *18*, 1065−1077.

(39) Goodson, D. Z.; Boyd, A. D., unpublished.

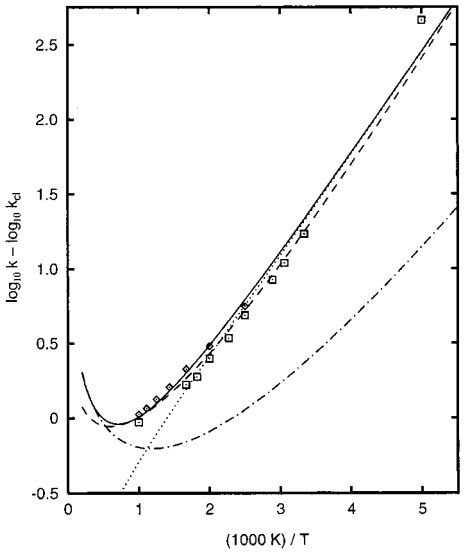

Figure 3. Difference between $\log_{10} k$ and $\log_{10} k_{cl}$ vs 1000 K/T for $H_2 + H \rightarrow H + H_2$, with k and k_{cl} in units of cm^3 molecule^{-1} s^{-1}. The units of k are cm^3 molecule^{-1} s^{-1}. Diamonds indicate results from quantum scattering theory,[31] while squares indicate flux autocorrelation function results.[33] The solid curve corresponds to EQPTST, using eqs 27 and 9 with $\gamma = 1.5$. The dotted and the dash−dot curves show the low- and high-temperature limits of EQPTST. The dashed curve corresponds to the simplified EQPTST expression given by eq 30 with prefactor $a = 1.35 \times 10^{-13}$ cm^3 K^{-1} molecule^{-1} s^{-1}.

value for other systems, this would probably not cause too much error in the rate constants, since T_0 for most molecules of interest will be much smaller than the H_2 value. Therefore, we will treat $\gamma = 1.5$ as a general result that will be reasonably accurate for arbitrary systems.

Figure 3 shows EQPTST results calculated with various approximations to eq 27 that put the prefactor in the standard form of eq 23. The low-T approximation fails above 600 K, while the high-T expression fails below 2000 K. However, the expression

$$k = aT \exp[-E_a(T_{eff}^{(1)})/RT] \qquad (30)$$

with a chosen so that k is equal to the full TST result at 1000 K, is in close agreement with the full expression over a very wide range of T. This is shown by the dashed curve in Figure 3. Equation 30 was constructed as a compromise between the low- and high-T limits. At lower values of T, the use of T^1 instead of $T^{-1/2}$ makes k slightly too small, while the use of $\gamma = 1$ instead of 1.5 makes k slightly too large. This cancellation of errors is excellent for $150 < T < 1500$ K. At very high T, the approximate expression will lie somewhat below the full expression, but this might actually yield a more accurate result for the true rate constant. TST in the limit of high T breaks down due to barrier recrossings, which causes the predicted rate constant to be higher than the actual rate constant. Variational TST partly corrects for this effect, and eq 30 at 1500 K yields a result (1.02×10^{-11} cm^3 molecule^{-1} s^{-1}) that is closer to the variational TST result of Garrett et al. (0.98×10^{-11} cm^3 molecule^{-1} s^{-1}) than is our full nonvariational TST result (1.05×10^{-11} cm^3 molecule^{-1} s^{-1}).

2. $CH_4 + H \rightarrow CH_3 + H_2$. This reaction will have the same limiting T dependence in the Arrhenius prefactor as $H_2 + H$, that is, $T^{-1/2}$ at low T and $T^{3/2}$ at high T. Therefore, the arguments that led to eq 30 should be valid as well for $CH_4 + H$. We obtained temperature-dependent activation energies as

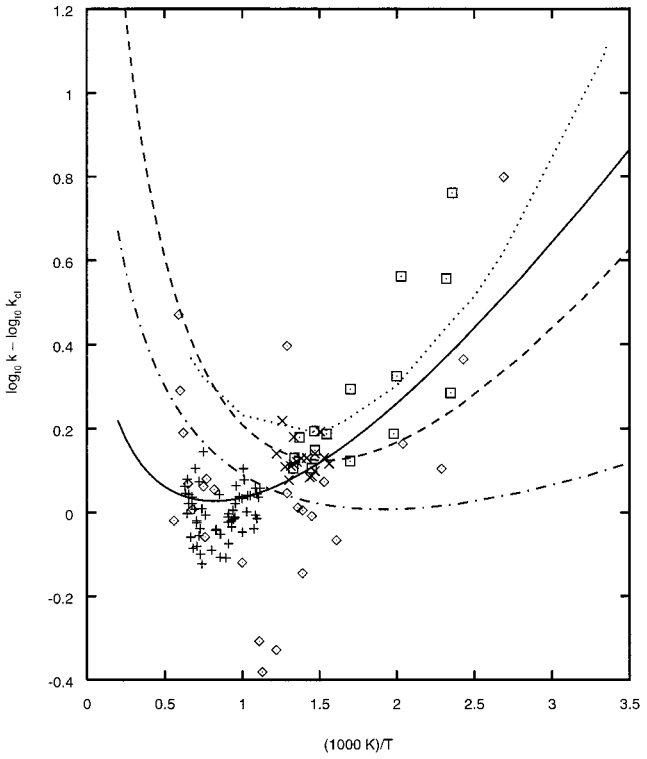

Figure 4. Difference between $\log_{10} k$ and $\log_{10} k_{cl}$ vs 1000 K/T for $CH_4 + H \rightarrow CH_3 + H_2$, with k and k_{cl} in units of cm^3 molecule^{-1} s^{-1}. k_{cl} is the is the rate constant from classical collision theory, eq 26, with temperature-independent E_a and prefactor $a = 3.65 \times 10^{-12}$ cm^3 K$^{-1/2}$ molecule^{-1} s^{-1}. The solid curve corresponds to the simplified EQPTST expression given by eq 30 with prefactor $a = 8.78 \times 10^{-14}$ cm^3 K^{-1} molecule^{-1} s^{-1}. The dotted curve corresponds to variational quantum TST.[17] The dashed and dash−dot curves show empirical fits from refs 2 and 3, respectively. The symbols indicate experimental points from the following references: Rabinowitz et al.[23] (+); Sepehrad et al.[19] (×); Kurylo et al.[21,22] (□); and various earlier studies reviewed by Shaw[12] (◇).

the difference between V_{eff} evaluated at the reactants well and at the CH_5 saddle point, using a linear C−H−H configuration. For the standard deviations σ_{HH} and σ_{CH}, the effective temperature function $T_{eff}^{(1)}$ was used. E_a is fit by the expression

$$E_a = 12.00 \text{ kcal mol}^{-1} - (1209 \text{ kcal mol}^{-1} K)(T + T_{0,CH})^{-1} + (7401 \text{ kcal mol}^{-1} K^{3/2})(T + T_{0,CH})^{-3/2} \quad (31)$$

within ±0.016 kcal/mol over the range $0 \le 1000K/T \le 3.5$. Equation 31 has the form of an expansion in terms of σ_{CH}. The calculation of the CH_5 energy uses σ_{CH} only for the integration over C−H bonds and σ_{HH} for the H−H bond. Nevertheless, a fit for E_a with T_0 treated as a free parameter yields $T_{0,CH}$ as very nearly the optimal value.

Experimental results for this reaction span a temperature range from 372 to almost 2000 K. TST studies[11−17] have predicted a distinct upward curvature in the Arrhenius plot, and a review by Shaw[12] of experimental results through the year 1978 supported this prediction. Subsequently, Sepehrad et al.[19] concluded that a linear Arrhenius plot was more consistent with the data, after omitting some apparently unreliable earlier results and adding new results of their own. More recent analyses by Baulch et al.[20] and by Rabinowitz et al.[23] discerned curvature with $A \propto T^3$ and $A \propto T^{2.11}$, respectively, while the GRI-Mech database for combustion modeling[3] currently uses $A \propto T^{1.62}$.

Figure 4 compares the experimental results for the rate constant with theoretical results and empirical fits. The experimental points correspond to (□) the ESR flow-tube studies of Kurylo et al.,[21,22] (×) the flow-discharge study of Sepehrad et al.,[19] (+) the flash-photolysis shock-tube study of Rabinowitz et al.,[23] and (◇) other miscellaneous earlier studies reviewed by Shaw.[12] (However, we have omitted the result from Rost and Just[40] on account of the critique of that study by Rabinowitz et al.[23]) The solid curve is our result from EQPTST using the simplified expression, eq 30, for the rate constant and eq 31 for the E_a, and with the prefactor chosen to agree with the full EQPTST result at 1000 K. The dashed and dash−dot curves show empirical fits that have recently been recommended for use in combustion modeling. The dashed curve comes from the expression given by Glassman[2] in the latest edition of his textbook. This expression is similar to the one recommended by Baulch et al.[20] The dash−dot curve corresponds to the expression in the GRI-Mech database.[3] Finally, the dotted curve shows the results of Truong's variational TST analysis with multidimensional semiclassical tunneling correction.[17]

Conclusion

Figure 4 shows that a simple analytical expression, eq 30, with a temperature-dependent activation energy determined from a Gaussian average of an empirical potential energy function gives good agreement with experimental rate constants for CH_4 + H over the full temperature range for which they are available. This is especially striking since none of the parameters in the expression were determined by fitting to the experimental points.

The approach presented here provides a middle ground between the purely empirical fits that are generally used in practical applications and the highly sophisticated, but computationally demanding, ab initio theoretical treatments. Since our method is based on an empirical potential energy surface, it is in essence an empirical fit. However, the empirical data set is not limited to the rate constants themselves. It includes, indirectly, the wide range of hydrocarbon properties such as molecular geometries and atomization energies used in the parametrization of the potential. (We have, in effect, augmented Brenner's original data set with the three parameters $T_{0,HH}$, $T_{0,CH}$, and γ.) We obtain analytic expressions that are not much more complicated than the standard empirical forms, but because they contain a much greater variety of empirical information, and because the functional form of the temperature dependence is justified theoretically, they can be expected to be more dependable at temperatures at which experimental results are unavailable. This is a significant advantage, since rate constants for reactions involving free radicals are difficult to measure experimentally, especially over the large temperature ranges that are needed for modeling the chemistry of the atmosphere and the extremely large temperature ranges needed to model such processes as pyrolysis and combustion.

In the present work, calculations were performed in the context of TST. Another approach to reaction rate calculations is direct simulation using molecular dynamics. The success of our EQPTST has two implications for such simulations. First, it supports the use[41] of the Brenner hydrocarbon potential in those studies. This is an empirical potential, parametrized to a data set consisting of properties of *stable* chemical species, yet judging from the success of our rate constant calculations it

(40) Rost, P.; Just, Th. *Ber. Bunsen-Ges. Phys. Chem.* **1975**, *79*, 682−686.

(41) Brenner, D. W.; Garrison, B. J. *Adv. Chem. Phys.* **1989**, *71*, 281−334. Garrison, B. J.; Dawnkaski, E. J.; Srivastava, D.; Brenner, D. W. *Science* **1992**, *255*, 835−838.

seems to be able to accurately model the unstable CH_5 transition state, since the curvature of the Arrhenius plot depends sensitively on the topography of the potential in the vicinity of the saddle point.

The second implication is that it might be possible to use a classical molecular dynamics calculation with a Gaussian-averaged effective potential in place of quantum dynamics to model processes in which quantum effects are important. The evaluation of the potential function is the most time-consuming step in a molecular dynamics simulation. Therefore, the use of numerical quadrature to perform the Gaussian averaging in such computations would be impractical. However, we are developing analytic expressions that approximate the necessary integrals so that the computational cost of calculating the potential will not be substantially increased.

In the present work our goal has been to develop approximations that put the path-integral expression for quantum dynamics in a form that requires only minor modifications of the usual classical dynamics approaches to reaction rate theory. If necessary, the effects of these approximations could be quantified (at the cost of additional computational expense) by using more rigorous path-integral methods.[7,25]

Acknowledgment. We thank David Golden, Andrew Boyd, and Dudley Herschbach for helpful discussions. This work was supported by the Welch Foundation and the National Science Foundation.

JA000674+